# Macromolecules 2018, 51, 6359–6368

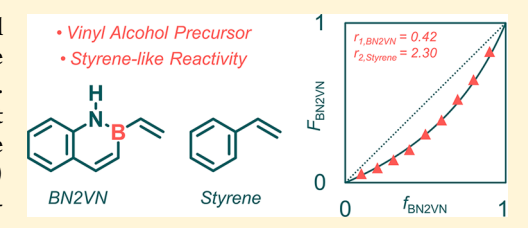
# An Organoborane Vinyl Monomer with Styrene-like Radical Reactivity: Reactivity Ratios and Role of Aromaticity

Heidi L. van de Wouw, Elorm C. Awuyah, Jodie I. Baris, and Rebekka S. Klausen\*

Department of Chemistry, Johns Hopkins University, 3400 N. Charles St., Baltimore, Maryland 21218, United States

Supporting Information

ABSTRACT: BN 2-vinylnaphthalene (BN2VN) is a novel precursor to vinyl alcohol copolymers via sodium hydroperoxide oxidation. We show that the unusual aromaticity of the BN heterocycle leads to styrene-like reactivity. Computational data including structural parameters and nucleus independent chemical shift (NICS) values support the aromaticity of the BN naphthalene side chain of BN2VN. Styrene (St) and BN2VN reactivity ratios ( $r_1$ (BN2VN) = 0.423;  $r_2(St) = 2.30$ ;  $r_1r_2 = 0.97$ ) were determined by nonlinear leastsquares (NLLS) statistical methods. We demonstrate control of copolymer



physical properties, including glass transition temperature. This work outlines design principles for the synthesis of tailored polymeric styrene-vinyl alcohol architectures.

#### ■ INTRODUCTION

Poly(vinyl alcohol) (PVA) is a widely used water-soluble coating and adhesive via cross-linking with boric acid. It is commercially synthesized by free radical polymerization of vinyl acetate (VAc), followed by hydrolysis. While PVA's physical properties such as solvent resistance, crystallinity, and toughness are in principle modulated by incorporation of nonpolar groups, the reactivity mismatch between VAc and conjugated monomers complicates the synthesis of hydroxyfunctionalized polymers by direct radical copolymerization.<sup>2–4</sup>

The copolymerization behavior of two monomers M1 and  $M_2$  is described by their reactivity ratios  $r_1$  and  $r_2$ , which indicate the propagation preference of each monomer (Scheme 1a). The reactivity ratio  $r_1$  is the ratio of the rate constants  $(k_{11}/k_{12})$  for addition of M<sub>1</sub> or M<sub>2</sub> to an M<sub>1</sub>-terminated polymer. Likewise, the reactivity ratio  $r_2$  is the ratio of the rate constants  $(k_{22}/k_{21})$  for addition of  $M_2$  or  $M_1$  to an  $M_2$ terminated polymer. A large reactivity ratio  $r_1$  indicates a strong preference for homopolymerization, while a reactivity ratio  $r_1$  significantly less than 1 indicates a strong preference for cross-polymerization. Ideal copolymerization is observed when the product of the reactivity ratios is 1.6

VAc and St are examples of an extremely mismatched comonomer pair in which the rate of cross-polymerization is essentially zero (Scheme 1b). The reactivity ratios  $r_1(VAc) =$ 0.01 and  $r_2(St) = 55$  indicate that both St- and VAc-terminated polymers strongly prefer to add St. Instead of copolymerization, consecutive homopolymerization is observed: St polymerizes first, and when consumed VAc homopolymerization is initiated. Indeed, minute St quantities on the order of the initiator concentration inhibit VAc polymerization by consuming all initiator.3 The structural dissimilarity of St and VAc contributes to the reactivity mismatch: while the St-terminated polymeric radical is significantly resonance stabilized, the VActerminated polymer is not.

We recently reported a solution to the challenging St-VAc radical copolymerization. The free radical copolymerization of St and BN 2-vinylnaphthalene (BN2VN), followed by sodium hydroperoxide (NaOOH) oxidation, provided statistical styrene-vinyl alcohol copolymers (Scheme 1c). 7,8 Evidence for a statistical copolymer includes the observation of a single glass transition temperature  $(T_g)$  intermediate between PBN2VN and polystyrene (PS) as well as a single  $T_{\sigma}$ intermediate between PVA and PS in oxidized samples.

BN2VN is a unique vinylborane due to the aromaticity of the 10  $\pi$ -electron BN naphthalene ring system (Scheme 1c). The Hückel aromaticity of cyclic conjugated BN materials<sup>9,10</sup> is well-established on the basis of resonance stabilization energy,  $^{11}$  electronic structure,  $^{12}$  and magnetic properties.  $^{12-15}$ Building on Sneddon's early work on vinylborazine (VB) polymerization, <sup>16–18</sup> several groups have recently explored BN for CC bond substitution in polymer backbones, 19-24 conjugated polymers, <sup>25-27</sup> or aromatic side chains. <sup>7,8,28,29</sup>

While in principle any organoborane is a precursor to PVA via oxidation, BN2VN is attractive in several respects. BN2VN is stable to benchtop handling, whereas many organoboranes are air- and water-sensitive and prone to cross-linking. 30,31 We attribute BN2VN's increased stability to the aromatic cage surrounding the central boron atom. A high-throughput twostep synthesis of BN2VN makes multigram scale polymerization possible. Monocyclic BN aromatic heterocycles currently require multistep syntheses, 9,32–35 which limits polymerizations to the milligram scale. 28,29 VB polymerization is hampered by polymer cross-linking arising from thermal dehydrogenative coupling of the inorganic side chain and hydrolytic instability. <sup>16,17,36</sup>

Received: June 27, 2018 Revised: July 26, 2018 Published: August 13, 2018

Scheme 1. (a) Reactivity Ratios for a Comonomer Pair  $M_1$  and  $M_2$ ; (b) Prior Work on the Synthesis of Styrene-Vinyl Alcohol Copolymers: Extreme Reactivity Mismatch between St and VAc or St and Vinylsilanes (VSi) Results in Zero or Low Hydroxy Content, While BN2VN Leads to High Hydroxy Content; (c) This Work: Hückel Aromaticity of BN Naphthalene and Determination of the Reactivity Ratios of St and BN2VN

BN2VN's aromaticity enables compatible reactivity with St and high copolymer hydroxy content. For example, while vinylsilanes are typically more bench stable than vinylboronates, these lack aromatic character. Inoue et al. reported an alkoxyvinylsilane monomer (VSi) for styrene copolymerization that yields vinyl alcohol derivatives after Tamao–Fleming oxidation. VSi incorporation is limited by mismatched reactivity ratios  $[r_1(VSi) = 0.11, r_2(St) = 20]$  (Scheme 1b). Section 15.

Herein we characterize BN2VN's aromaticity and measure well-matched St and BN2VN reactivity ratios by traditional linearization methods and modern nonlinear least-squares methods (NLLS:  $r_1(BN2VN) = 0.423$ ,  $r_2(St) = 2.30$ ;  $r_1r_2 = 0.97$ ). Quantitative assessment of BN2VN and St reactivities enables fine control of copolymerization and the design of tailored styrene—vinyl alcohol copolymers.

# **■ EXPERIMENTAL SECTION**

**Computational Methods.** Density functional theory (DFT) calculations were performed using the Gaussian 09 program package. Geometries were optimized using the restricted or unrestricted CAM-B3LYP³9 hybrid exchange-correlation functional with the 6-311G-(d,p) basis set. CAM-B3LYP is known to reliably describe radicals and extended conjugated systems. <sup>40,41</sup> Frequency calculations performed at the same level of theory on fully optimized geometries showed no imaginary frequencies, confirming optimized geometries as local minima on their potential surfaces. Energies reported are the sum of electronic and thermal enthalpies at 298.15 K and are converted to kcal mol $^{-1}$  from hartrees (1  $E_{\rm h}=627.509608~{\rm kcal~mol}^{-1}$ ). Visualization of optimized geometries and electrostatic potential (ESP) maps were performed using GaussView 5.0.9.

Nucleus-independent chemical shifts (NICS) were calculated as the negative value of the nuclear magnetic shielding computed at the geometric center of the rings (NICS(0)) and 1.0 Å above the geometric center of the rings (NICS(1)) by the gauge-independent atomic orbital (GIAO) method.  $^{54-58}$ 

Homolytic bond dissociation energies (BDEs) are calculated as follows: BDE =  $(E_{rs} + E_{Ha}) - E_{cs}$ , where  $E_{rs}$  is the enthalpy corrected energy of the radical species,  $E_{Ha}$  is the energy of a hydrogen atom, and  $E_{cs}$  is the enthalpy corrected energy of the closed shell species.

General Procedure for Copolymer Synthesis. Stock solutions of St and BN2VN (3.00 M in toluene) and AIBN (31.2 mg/mL in toluene) were prepared. In a nitrogen atmosphere glovebox, monomers (10.00 mmol total) and AIBN (0.095 mmol) were added to microwave reaction vials, and the vials were sealed. The sealed vials were heated in a preheated pie plate at 70 °C for 45 min with vigorous stirring. Upon opening to air, solutions were immediately transferred to a beaker of methanol (80 mL). The microwave vial was rinsed with dichloromethane (2  $\times$  1 mL) and rinsates added to the methanol. Precipitated polymer was isolated by filtration through a thin pad of Celite (~3–5 mm), washed with methanol (10 mL), and then eluted with dichloromethane (2  $\times$  5 mL). Methanol precipitation was repeated a second time. The purified polymer was dried in a vacuum oven for about 18 h at 85 °C.

 $P(BN2VN_4\text{-}co\text{-}S_{103})$ . Synthesized according to the general procedure using BN2VN (0.33 mL, 1.00 mmol) and St (3.00 mL, 9.00 mmol) to yield a white powder (yield 67.3 mg, 6.2%). <sup>1</sup>H NMR (400 MHz, CD<sub>2</sub>Cl<sub>2</sub>, δ): 8.01–6.18 (br, 4.83 H), 2.77–0.44 (br, 3.00 H). FTIR (KBr, thin film)  $\nu_{\text{max}}$ : 3060 (m), 3026 (m), 2924 (m), 2850 (w), 1601 (w), 1560 (w), 1493 (m), 1452 (m), 1028 (w), 759 (m), 698 (s), 541 (w) cm<sup>-1</sup>.

 $P(BN2VN_{10}\text{-}co\text{-}S_{86})$ . Synthesized according to the general procedure using BN2VN (0.667 mL, 2.00 mmol) and St (2.67 mL, 8.00 mmol)

to yield a white powder (yield 74.6 mg, 6.5%).  $^{1}$ H NMR (400 MHz, CD<sub>2</sub>Cl<sub>2</sub>,  $\delta$ ): 8.02–6.15 (br, 4.87 H), 2.80–0.34 (br, 3.00 H). FTIR (KBr, thin film)  $\nu_{\text{max}}$ : 3059 (w), 3025 (m), 2923 (m), 2849 (w), 1615 (m), 1562 (m), 1493 (m), 1452 (m), 806 (w), 760 (m), 689 (s), 541 (w) cm<sup>-1</sup>.

 $P(BN2VN_{15}\text{-}co\text{-}S_{81})$ . Synthesized according to the general procedure using BN2VN (1.00 mL, 3.00 mmol) and St (2.33 mL, 7.00 mmol) to yield a white powder (yield 62.2 mg, 5.2%). <sup>1</sup>H NMR (400 MHz, CD<sub>2</sub>Cl<sub>2</sub>, δ): 8.01–6.06 (br, 4.99 H), 2.75–0.45 (br, 3.00 H). FTIR (KBr, thin film)  $\nu_{\text{max}}$ : 3059 (w), 3025 (m), 2923 (br), 2848 (w), 1615 (m), 1598 (m), 1563 (m), 1493 (m), 1452 (m), 761 (m), 698 (s) cm<sup>-1</sup>.

 $P(BN2VN_{20}\text{-}co\text{-}S_{70})$ . Synthesized according to the general procedure using BN2VN (1.33 mL, 4.00 mmol) and St (2.00 mL, 6.00 mmol) to yield a white powder (yield 66.5 mg, 5.3%). <sup>1</sup>H NMR (400 MHz, CD<sub>2</sub>Cl<sub>2</sub>, δ): 8.01–6.05 (br, 5.03 H), 2.79–0.39 (br, 3.00 H). FTIR (KBr, thin film)  $\nu_{\text{max}}$ : 3059 (w), 3025 (m), 2920 (br), 2847 (w), 1614 (m), 1597 (w), 1563 (m), 1493 (m), 1452 (m), 1439 (m), 806 (w), 761 (m), 698 (s) cm<sup>-1</sup>.

*P(BN2VN*<sub>25</sub>-co-S<sub>61</sub>). Synthesized according to the general procedure using BN2VN (1.67 mL, 5.00 mmol) and St (1.67 mL, 5.00 mmol) to yield a white powder (yield 63.8 mg, 4.9%). <sup>1</sup>H NMR (400 MHz, CD<sub>2</sub>Cl<sub>2</sub>, δ):8.04–6.08 (br, 5.13 H), 2.84–0.39 (br, 3.00 H). FTIR (KBr, thin film)  $\nu_{\rm max}$ : 3372 (br), 3059 (w), 3025 (m), 2918 (br), 2847 (w), 1614 (m), 1596 (w), 1562 (m), 1540 (w), 1493 (m), 1452 (m), 1438 (m), 1387 (w), 1345 (w), 1137 (m), 806 (m), 761 (s), 699 (s), 458 (m) cm<sup>-1</sup>.

*P*(*BN2VN*<sub>32</sub>-*co*-5<sub>46</sub>). Synthesized according to the general procedure using BN2VN (2.00 mL, 6.00 mmol) and St (1.33 mL, 4.00 mmol) to yield a white powder (yield 63.7 mg, 4.7%). <sup>1</sup>H NMR (400 MHz, CD<sub>2</sub>Cl<sub>2</sub>, δ): 8.11–5.90 (br, 5.28 H), 2.79–0.36 (br, 3.00 H). FTIR (KBr, thin film)  $\nu_{\rm max}$ : 3373 (br), 3058 (w), 3025 (m), 2915 (br), 2845 (w), 1614 (m), 1596 (m), 1562 (s), 1493 (m), 1451 (m), 1439 (m), 806 (m), 760 (s), 699 (s), 458 (m) cm<sup>-1</sup>.

 $P(BN2VN_{38}\text{-}co\text{-}S_{35}\text{)}$ . Synthesized according to the general procedure using BN2VN (2.33 mL, 7.00 mmol) and St (1.00 mL, 3.00 mmol) to yield a white powder (yield 47.6 mg, 3.4%). <sup>1</sup>H NMR (400 MHz, CD<sub>2</sub>Cl<sub>2</sub>, δ): 8.03–6.10 (br, 5.40 H), 2.60–0.38 (br, 3.00 H). FTIR (KBr, thin film)  $\nu_{\text{max}}$ : 3373 (br), 3025 (m), 2911 (br), 2844 (w), 1614 (s), 1596 (m), 1562 (s), 1493 (m), 1438 (s), 1137 (w), 806 (m), 760 (s), 700 (s), 458 (m) cm<sup>-1</sup>.

 $P(BN2VN_{41}\text{-}co\text{-}S_{20})$ . Synthesized according to the general procedure using BN2VN (2.67 mL, 8.00 mmol) and St (0.667 mL, 2.00 mmol) to yield a white powder (yield 55.7 mg, 3.8%). <sup>1</sup>H NMR (400 MHz, CD<sub>2</sub>Cl<sub>2</sub>, δ): 8.10–5.95 (br, 5.55 H), 2.66–0.33 (br, 3.00 H). FTIR (KBr, thin film)  $\nu_{\text{max}}$ : 3375 (br), 3024 (m), 2903 (br), 2842 (m), 1614 (s), 1597 (m), 1562 (s), 1492 (m), 1472 (m), 1439 (s), 1136 (m), 806 (m), 761 (s), 700 (m), 459 (m) cm<sup>-1</sup>.

*P*(*BN2VN*<sub>39</sub>-*co*-*S*<sub>11</sub>). Synthesized according to the general procedure using BN2VN (3.00 mL, 9.00 mmol) and St (0.333 mL, 1.00 mmol) to yield a white powder (yield 57.9 mg, 3.9%). <sup>1</sup>H NMR (400 MHz, CD<sub>2</sub>Cl<sub>2</sub>, δ): 8.07–5.87 (br, 6.58 H), 2.50–0.30 (br, 3.00 H). FTIR (KBr, thin film)  $\nu_{\text{max}}$ : 3375 (br), 3024 (w), 2897 (br), 2841 (m), 1614 (s), 1596 (m), 1562 (s), 1474 (m), 1438 (s), 1136 (m), 806 (m), 760 (s), 700 (m), 458 (m) cm<sup>-1</sup>.

**Statistical Methods.** Experimental data derived from UV—vis spectroscopy and elemental analysis were fit using the NLLS method with Contour version 1.8 with 3% and 1% relative estimated error, respectively. Point estimates of the reactivity ratios and a 95% joint confidence interval were calculated.

# ■ RESULTS AND DISCUSSION

**Molecular Geometries.** Calculations on BN2VN reveal structural signatures of aromaticity including ring planarity and bond lengths intermediate between single and double bonds. Geometries were optimized using the restricted or unrestricted CAM-B3LYP<sup>39</sup> hybrid exchange-correlation functional with the 6-311G(d,p) basis set. CAM-B3LYP is known to reliably describe radicals and extended conjugated systems. 40,41

Geometry optimization of St and BN styrene (BNSt) as control structures was performed at the same level of theory.

All three geometry-optimized structures are planar, as seen in top-down and side-on views (Figure 1). In BN2VN, the sum

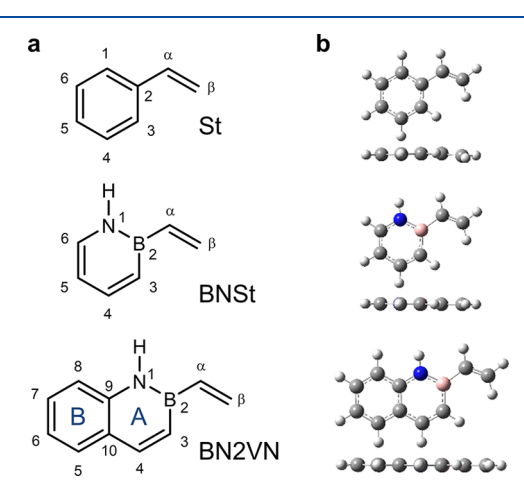


**Figure 1.** (a) Chemical structures of St, BNSt, and BN2VN with atom and ring numbering indicated. BN naphthalene numbering adapted from Dewar and Liu.  $^{42,43}$  (b) Geometry-optimized structures (CAM-B3LYP/6-311G(d,p)). Top-down and side-on views highlight planarity.

of the bond angles within both the A and B rings of BN2VN is  $720^{\circ}$  and the average bond angle is  $120^{\circ}$  (Table 1). The same

Table 1. Range of Endocyclic Bond Angles (deg) in St, BNSt, and BN2VN (from Geometry-Optimized Structures)

	St	BNSt	BN2VN
minimum	118.1	114.0	114.7 (A ring) 118.6 (B ring)
maximum	121.2	123.9	125.0 (A ring) 121.4 (B ring)
average	120.0	120.0	120.0 (A ring) 120.0 (B ring)
sum	720.0	720.0	720.0 (A ring) 720.0 (B ring)

is observed in St and BNSt. The BN rings have a wider range of bond angles than the all carbon systems, reflecting the lower aromaticity of BN benzene (1,2-azaborine) analogues.

Optimized bond lengths are shown in Table 2. The BN bond in BN2VN is 1.422 Å. This value is consistent with the calculated BN bond length in BNSt (1.434 Å), 1,2-azaborine (1.438 Å), 14 and other previous theoretical work. 44,45 The calculated BN bond length in BN2VN and BNSt is intermediate between BN single (1.582 Å) 46 and double bonds (1.396 Å). 47–49 The CC bonds are also intermediate between single and double bonds in length. A wider range of bond lengths is observed in BN aromatic rings than in all carbon rings.

The  $C(\alpha)$ – $C(\beta)$  bond lengths in BNSt and BN2VN are both predicted to be 1.331 Å long, on par with a typical C–C double bond (1.34 Å). Vinyl bond lengths between 1.317 and 1.326 Å are reported in crystal structures of related neutral B-vinyl compounds, supporting the validity of the predicted bond lengths. <sup>50,51</sup>

Crystal structures of the vinyl monomers are not available to confirm the predicted bond lengths. BNSt is a volatile liquid. While we successfully grew large colorless plate-like crystals of BN2VN, diffraction was surprisingly poor as crystals barely diffracted beyond 1 Å (using both Mo and Cu K $\alpha$  radiation).

Table 2. Selected Bond Lengths (Å) in St, BNSt, and BN2VN (from Geometry-Optimized Structures; See Figure 1 for Atom Numbering)

St		BNSt		BN2VN	Г
C(1)-C(2)	1.395	B-N	1.434	B-N	1.422
C(2)-C(3)	1.397	B-C(3)	1.516	B-C(3)	1.530
C(3)-C(4)	1.384	C(3)-C(4)	1.363	C(3)-C(4)	1.350
C(4)-C(5)	1.390	C(4) - C(5)	1.424	C(4)-C(10)	1.442
C(5)-C(6)	1.386	C(5)-C(6)	1.356	C(10)-C(9)	1.408
C(6)-C(1)	1.387	C(6)-N	1.363	C(9)-N	1.380
$C(\alpha)-C(\beta)$	1.328	$C(\alpha)-C(\beta)$	1.331	$C(\alpha)-C(\beta)$	1.331

Several attempts to collect data at different temperatures (110, 200, and 293 K) were carried out, but all lead to poor quality diffraction patterns. Strong decay of intensities at higher resolution may be explained by poor long-range order in the crystal.

NICS Calculations. Nucleus-independent chemical shift (NICS) calculations<sup>52,53</sup> are routinely used as a magnetic index of local aromaticity. NICS values give a quantitative correlation of aromaticity by computing magnetic shielding or deshielding of a ghost atom (Bq) at ring centers or any location of interest. The location of Bq influences the magnitude of the shielding or deshielding effect arising from ring current. Significantly negative NICS values denote aromaticity and diatropic ring currents, while significantly positive NICS values denote antiaromaticity and paratropic ring currents. NICS values close to 0 indicate a nonaromatic structure.

NICS values for BN2VN and several control structures were calculated as the negative value of the nuclear magnetic shielding computed at the geometric center of a ring (NICS(0)) and 1.0 Å above the geometric center of a ring (NICS(1)) by the gauge-independent atomic orbital (GIAO) method (Table 3). St exhibits the largest negative NICS values, while vinylborazine (VB) has the least negative NICS values. BNSt and BN2VN, in which only one CC bond is substituted with a BN bond, are intermediate between these structures. The A-ring of BN2VN is less aromatic than the B-

Table 3. Electrostatic Potential (ESP) Maps and NICS Comparisons (ppm) of Vinyl Monomers [10 kcal mol<sup>-1</sup> (Red) to 70 kcal mol<sup>-1</sup> (Blue)]

Structure	ESP Map	NICS(0) A ring	NICS(1) A ring	NICS(0) B ring	NICS(1) B ring
		-8.24	-10.78	-	-
I - N B		-4.53	-6.56	-	-
H H N B		-3.22	-5.83	-9.62	-11.25
H - N - N - H		-1.68	-2.63	-	-

ring but comparable to BNSt. Our results are consistent with prior computational work showing decreasing aromaticity with increasing BN substitution.  $^{13,14,45,59-61}$  The weak aromaticity of borazine  $(B_3N_3H_6)$  is attributed to the greater polarity of the BN bond compared to the CC bond, which localizes electron density on the more electronegative N atom.  $^{62,63}$ 

Electrostatic potential (ESP) maps support our conclusions about relative aromaticity. The poor delocalization of electrons in VB is readily apparent from its ESP map: electron density is highly localized to the electronegative nitrogen atoms. BN2VN exhibits the characteristic polarization of aromatic compounds, with an electron-deficient C-H edge and electron-rich surface above the plane of the ring. Electron density is less uniformly distributed above the  $\pi$  face in BNSt and BN2VN than in St.

**Bond Dissociation Energies.** Relative trends in hydrocarbon C–H bond dissociation energies correlate with radical stability. The weakest C–H bond in toluene accurately predicts that the most stable radical is formed at the benzylic position (Figure 2a). We investigated if BN aromatic rings exert a similar influence on bond dissociation energies as phenyl rings.

a
$$CH_3 \xrightarrow{BDE} CH_3 + H$$

BDE =  $[E(radical) + E(H \cdot)] - E(toluene)$ 

**Figure 2.** (a) BDE calculation, shown for the homolytic abstraction of a benzylic hydrogen atom from toluene. Energies used are the "sum of electronic and thermal enthalpies" terms from vibrational frequency job outputs. (b) Calculated BDEs for each indicated C–H or N–H bond for ethylbenzene (EtB), BN ethylbenzene (BNEtB), and BN 2-ethylnaphthalene (BN2EtN) (CAM-B3LYP/6-311G(d,p)).

We selected BN 2-ethylnaphthalene (BN2EtN) as a model system. Ethylbenzene (EtB) and BN 2-ethylbenzene (BNEtB) are included for comparison. Vibrational frequencies of fully geometry-optimized closed shell and radical structures were computed using the CAM-B3LYP functional with the 6-311G(d,p) basis set. From these data, theoretical gas phase bond dissociation enthalpies (BDEs,  $\Delta_{rxn}H_{298}$ ) were calculated

**Table 4. Copolymer Properties** 

entry	sample name <sup>a</sup>	yield (%)	$M_{\rm n}^{\ b}$ (kDa)	$M_{\rm w}/M_{\rm n}^{b}$	$f_{ m BN2VN}$	$\epsilon_{320}^{c}$	$F_{\rm BN2VN}^{d}$ (UV-vis)	$F_{\rm BN2VN}^{e}$ (EA)
1	$P(BN2VN_4$ -co- $S_{103})$	6.2	11.4	1.48	0.100	1.90	0.0411	0.0568
2	$P(BN2VN_{10}\text{-}co\text{-}S_{86})$	6.5	10.4	1.50	0.200	4.26	0.101	0.0965
3	$P(BN2VN_{15}$ -co- $S_{81})$	5.2	10.8	1.53	0.300	6.44	0.160	0.148
4	$P(BN2VN_{20}\text{-}co\text{-}S_{70})$	5.3	10.4	1.48	0.400	8.59	0.221	0.213
5	$P(BN2VN_{25}\text{-}co\text{-}S_{61})$	4.9	10.3	1.48	0.500	10.9	0.292	0.309
6	$P(BN2VN_{32}\text{-}co\text{-}S_{46})$	4.7	9.63	1.46	0.600	14.5	0.409	0.395
7	$P(BN2VN_{38}\text{-}co\text{-}S_{35})$	3.4	9.53	1.44	0.700	17.5	0.516	0.521
8	$P(BN2VN_{41}\text{-}co\text{-}S_{20})$	3.8	8.39	1.38	0.800	21.5	0.675	0.643
9	$P(BN2VN_{39}\text{-}co\text{-}S_{11})$	3.9	7.22	1.34	0.900	23.9	0.779	0.819

"Samples are named according to average degree of polymerization ( $\overline{DP}$ ) of each monomer. See the Supporting Information for details. Determined by GPC analysis at 254 nm relative to a polystyrene standard. In L g<sup>-1</sup> cm<sup>-1</sup>. Determined by UV—vis from  $\varepsilon_{320}$  according to eq 4. Determined by elemental analysis (EA) from wt % C according to eq 5.

at 298.15 K from homolytic cleavage of various C-H and N-H bonds from enthalpy corrected energies (Figure 2a). 66,67

The calculated C–H BDEs of BN2EtN follow the trends consistent with our intuitive understanding of radical stabilization effects in hydrocarbons (Figure 2b). The  $C(\alpha)$ –H bond has the lowest BDE (87.3 kcal mol<sup>-1</sup>), followed by the  $C(\beta)$ –H bond (96.6 kcal mol<sup>-1</sup>). The aryl C–H bonds are significantly stronger (106–111 kcal mol<sup>-1</sup>) than alkyl C–H bonds, as is the N–H bond (109 kcal mol<sup>-1</sup>). Qualitatively similar trends are observed with EtB and BNEtB where the BDE decreases in the order  $\alpha < \beta <$  aryl (Figure 2b).

Carbon-centered alkyl radicals such as the  $\alpha$ -cyanoisopropyl radical derived from AIBN or benzylic radicals arising from toluene (PhCH<sub>2</sub>•) exclusively add to the tail position of styrene. The calculated BDE's suggest that there is no energetic reason to expect an increase in head addition or aromatic substitution with BN2VN.

**Reactivity Ratios: Linearization.** Reactivity ratios for radical copolymerizations following the terminal model are traditionally calculated by linearization of the copolymer equation (eq 1) where  $f_1$  is the mole fraction of  $M_1$  in the feed,  $f_2 = 1 - f_1$ ,  $F_1$  is the mole fraction of  $M_2$  in the copolymer, and  $F_2$  is the mole fraction of  $M_2$  in the copolymer.

$$F_{1} = \frac{r_{1}f_{1}^{2} + f_{1}f_{2}}{r_{1}f_{1}^{2} + 2f_{1}f_{2} + r_{2}f_{2}^{2}}$$
(1)

However, several assumptions underlying the linearization methods introduce significant systemic error, resulting in highly variable estimates of copolymerization reactivity ratios. <sup>69,70</sup> Nonlinear least-squares (NLLS) fitting is the most statistically accurate method for estimating reactivity ratios. <sup>71</sup> We describe initial estimation of St and BN2VN reactivity ratios based on the Fineman–Ross and Kelen–Tüdös linearization methods and then a NLLS analysis of the copolymerization data. Good agreement is observed between the three methods.

In the Fineman–Ross<sup>72</sup> method (eq 2) for linearization of the copolymer equation, several copolymerizations with different ratios of the two monomers are carried out to low conversion, and the composition of the copolymers is determined.

$$\frac{f_1(2F_1 - 1)}{(1 - f_1)F_1} = \frac{f_1^2(1 - F_1)}{(1 - f_1)^2F_1}r_1 - r_2$$
(2)

A plot of G versus H yields a straight line with slope  $r_1$  and y-intercept  $-r_2$ , where G and H are

$$G = \frac{f_1(2F_1 - 1)}{F_1(1 - f_1)}$$

$$H = \frac{f_1^2 (1 - F_1)}{(1 - f_1)^2 F_1}$$

A disadvantage of the Fineman–Ross method is that low or high values of  $f_1$  disproportionately influence the analysis. The Kelen–Tüdös method addresses this limitation by adding an arbitrary correction factor  $\alpha$  that uniformly distributes data points. The reactivity ratios  $r_1$  and  $r_2$  are determined by a fit of the experimental data to eq 3

$$\eta = [r_1 + (r_2/\alpha)]\xi - (r_2/\alpha)$$
(3)

where  $\eta$ ,  $\xi$ , and  $\alpha$  are

$$\eta = \frac{G}{\alpha + H}$$

$$\xi = \frac{H}{\alpha + H}$$

$$\alpha = \sqrt{H_{\min}H_{\max}}$$

The plot of  $\eta$  versus  $\xi$  gives a straight line with intercepts  $-r_2/\alpha$  and  $r_1$  when  $\xi=0$  and  $\xi=1$ , respectively.

Copolymerization of BN2VN and St  $(f_1/f_2 = 0.111-9.00)$  was performed with 2,2'-azobis(2-methylpropionitrile) (AIBN) as the radical initiator at 70 °C in toluene for 45 min. Polymerizations were quenched at low conversion (3–7%) by precipitation into methanol. Copolymer composition was analyzed by two independent techniques: absorbance spectroscopy and elemental analysis.

As previously reported, the unique absorbance at 320 nm of the BN naphthalene chromophore enables a UV–vis assay for quantitative determination of BN2VN content in a copolymer. The absorption at 320 nm is measured for a series of different blends of PS and PBN2VN. A plot of the extinction coefficient at 320 nm ( $\varepsilon_{320}$ ) versus the weight fraction of PBN2VN in the blend ( $X_{\rm BN2VN}$ ) is a straight line and linear regression provides eq 4 (Figure S1).

$$\chi_{\text{BN2VN}} = \frac{\varepsilon_{320} - 0.208}{28.2} \tag{4}$$

The fractional composition of BN2VN in a copolymer is calculated using eq 4 from the copolymer's extinction coefficient at 320 nm ( $\varepsilon_{320}$ ). UV—vis spectra of copolymer solutions were recorded in THF at room temperature (Figure S2).

BN2VN composition can also be determined by elemental analysis (Figure S3). Equation 5 describes the relationship between weight percent of carbon (wt % C) in a copolymer and the weight fraction BN2VN.

$$\chi_{\rm BN2VN} = -\frac{\text{wt } \% \text{ C} - 92.3}{14.8} \tag{5}$$

Table 4 summarizes copolymer characteristics. Good agreement is observed between both analytical methods with respect to determination of  $F_{\rm BN2VN}$ , the fractional composition of BN2VN in the copolymer.

Reactivity ratios determined using the Fineman-Ross method (Figure 3a) and the Kelen-Tüdös method (Figure

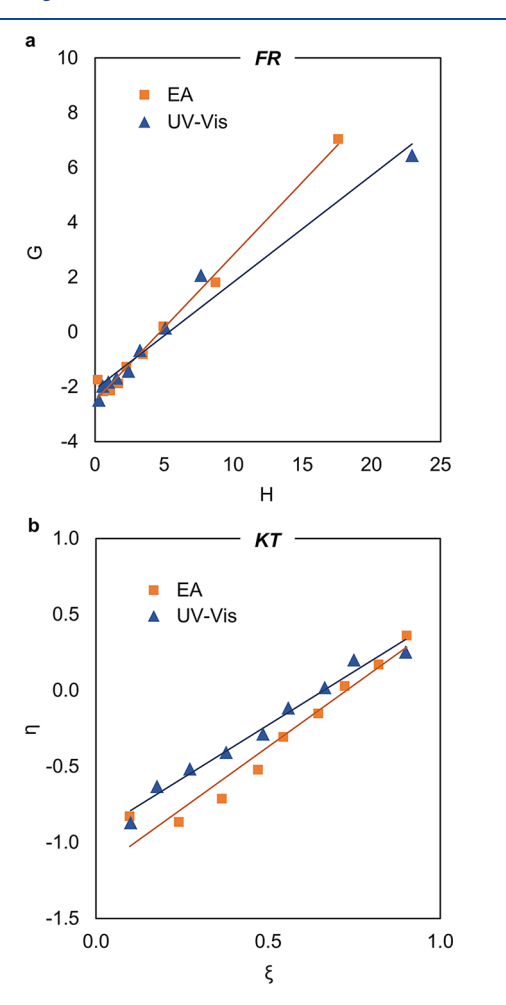


Figure 3. Determination of reactivity ratios for the copolymerization of BN2VN and St by the (a) Fineman–Ross (FR) method and (b) Kelen–Tüdös (KT) method.

3b) support an ideal radical copolymerization ( $r_1r_2 = 1$ ) in which St is somewhat more reactive than BN2VN. Four separate estimates of the reactivity ratios are obtained by analysis of each set of experimental data by both linearization methods (Table 5). In all cases,  $r_1(BN2VN)$  is close to 0.5 (0.390–0.531),  $r_2(St)$  is close to 2 (2.09–2.50), and the

product of the reactivity ratios  $(r_1r_2)$  is close to 1.0 (0.815–1.33).

**Reactivity Ratios: NLLS Analysis.** The Mayo–Lewis plots of the fractional composition of BN2VN in the copolymer  $(F_{\rm BN2VN})$  versus the fractional composition of BN2VN in the monomer feed  $(f_{\rm BN2VN})$  for both analytical methods are shown in Figures 4a,b. The dashed line indicates the linear behavior expected from a random (Bernoullian) copolymerization in which both monomers are equally reactive  $(r_1 = r_2 = 1)$ . Data analysis by van Herk's NLLS method<sup>71</sup> yielded estimates of the reactivity ratios  $r_1({\rm BN2VN})$  and  $r_2({\rm St})$  and a 95% joint confidence interval (JCI, Figure 4c,d). Point estimates of the reactivity ratios derived from linearization methods are included and fall within the confidence interval, with the exception of Fineman–Ross reactivity ratios derived from UV–vis spectroscopy.

On the basis of the NLLS data analysis, we report  $r_1(\mathrm{BN2VN}) = 0.517$  and  $r_2(\mathrm{St}) = 2.46$  (UV-vis) and  $r_1(\mathrm{BN2VN}) = 0.423$  and  $r_2(\mathrm{St}) = 2.30$  (EA). This is a dramatic narrowing of the difference in reactivity between styrene and a vinyl alcohol precursor compared to prior state of the art (Table 5).

**Polymer Microstructure.** The BN2VN and St reactivity ratios ( $r_1 < 1 < r_2$ ;  $r_1r_2 = 1$ ) belong to the special case of an ideal copolymerization in which the monomers do not have equal reactivities. An ideal copolymerization occurs when the propagating species has no preference for one monomer over another and implies that the product of the reactivity ratios  $r_1r_2$  must be 1 ( $k_{11} = k_{21}$  and  $k_{22} = k_{12}$ ).

$$r_1 r_2 = \frac{k_{11}}{k_{12}} \frac{k_{22}}{k_{21}} = 1$$

A subset of ideal copolymerizations occurs when  $r_1 = r_2 = 1$  (both monomers are equally reactive) and a random copolymer with an equal distribution of monomers results. An ideal copolymerization is still possible with monomers with unequal reactivities  $(r_1 < 1 < r_2)$ . In this case, at low conversion, a statistical copolymer is expected that is enriched in the more reactive monomer (e.g., St).

The glass transition temperature  $(T_{\rm g})$  is a probe of copolymer microstructure. A diblock copolymer has two  $T_{\rm g}$ 's corresponding to the homopolymer  $T_{\rm g}$ , while a statistical copolymer has a single  $T_{\rm g}$  intermediate between the homopolymers. A gradient copolymer has a single  $T_{\rm g}$ , typically wider than the homopolymers. While  $^{13}{\rm C}$  NMR spectroscopy is typically used for copolymer sequence analysis, the relaxation rate of the quadrupolar boron-11 nucleus (I=3/2) negatively influences the  $^{13}{\rm C}$  NMR signals of boron-adjacent carbon atoms, resulting in a drastic reduction in signal height.  $^{74}$ 

 $T_{\rm g}$ 's of the St-BN2VN copolymers were determined by differential scanning calorimetry (DSC) under nitrogen (Figure 5a). All copolymers show a single narrow  $T_{\rm g}$  intermediate between PS<sub>159</sub> ( $T_{\rm g}=96$  °C,  $M_{\rm n}=16.5$  kDa)<sup>78</sup> and PBN2VN<sub>132</sub> ( $T_{\rm g}=135.2$  °C,  $M_{\rm n}=20.4$  kDa),<sup>8</sup> which increases with increasing BN2VN content (Figure 5a). Good agreement is observed between experimental  $T_{\rm g}$ 's (triangles) and predicted  $T_{\rm g}$  (dashed line, Figure 5b and Table 7).<sup>76</sup> Minor deviations from prediction ( $\pm 7$  °C) may reflect the lower molecular weights of the samples in this study ( $M_{\rm n}=7.22-11.4$  kDa) compared to the PBN2VN reference and instrumental error (3–10 °C at a heating rate of 10 °C min<sup>-1</sup>).<sup>77</sup>

Table 5. Reactivity Ratios from Linearization Methods

	Fineman-Ross		Kelen-Tüd		
	elemental analysis	UV-vis	elemental analysis	UV-vis	average
$r_1(BN2VN)$	0.531	0.390	0.445	0.477	$0.461 \pm 0.06$
$r_2(St)$	2.50	2.09	2.25	2.39	$2.31 \pm 0.18$
$r_1r_2$	1.33	0.815	1.00	1.14	$1.07 \pm 0.22$

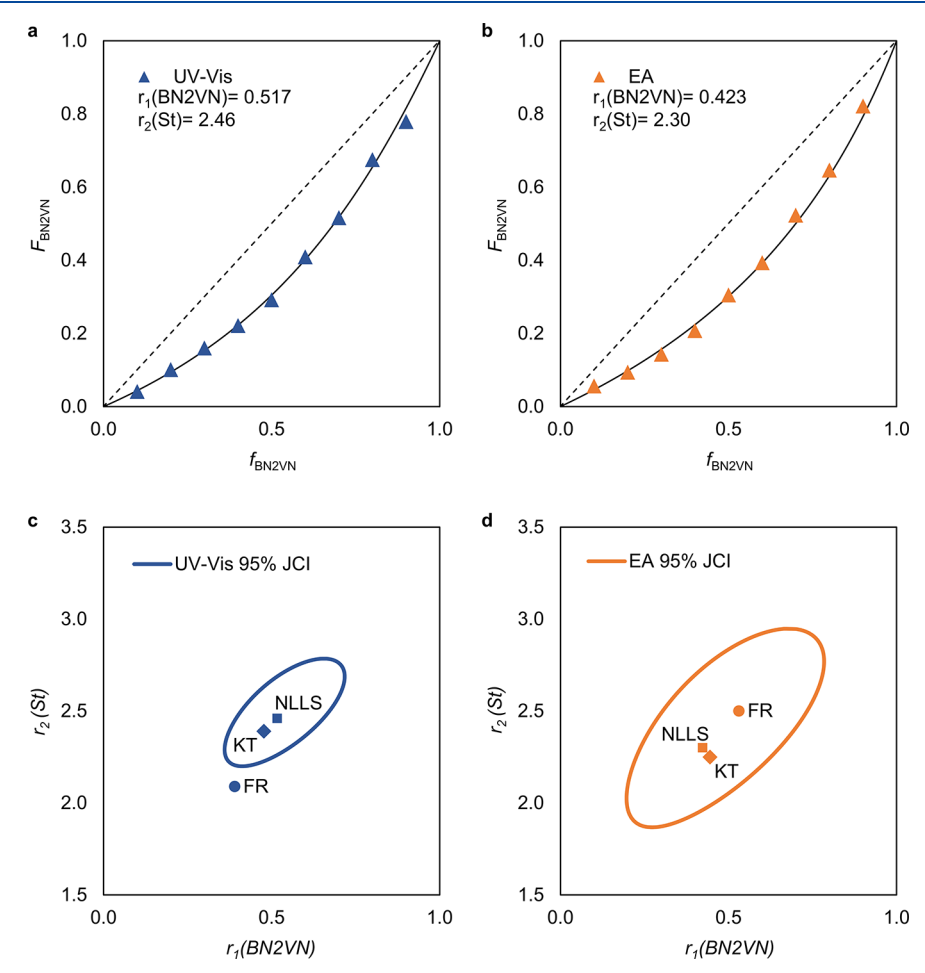


Figure 4. Mayo—Lewis plots of the fractional composition of BN2VN in the copolymer ( $F_{\rm BN2VN}$ ) versus the fractional composition of BN2VN in the monomer feed ( $f_{\rm BN2VN}$ ) determined by (a) UV—vis spectroscopy and (b) elemental analysis. The dashed line indicates the linear behavior expected from a random copolymerization ( $r_1 = r_2 = 1$ ); the solid line indicates behavior for the respectively labeled reactivity ratios. NLLS determined 95% joint confidence intervals (JCI's) and point estimates of the reactivity ratios derived by NLLS and linearization methods from (c) UV—vis and (d) elemental analysis data.

Table 6. Comparison of Reactivity Ratios in the Copolymerization of St and a Vinyl Alcohol Precursor

entry	vinyl alcohol precursor	$r_1$ (precursor)	$r_2(\mathrm{St})$	reference
1	VAc	0.01	55	2
2	VSi	0.11	20	38
3	BN2VN	0.42 (EA) 0.52 (UV-vis)	2.3 (EA) 2.5 (UV-vis)	this work

Characterization is consistent with the predicted St-enriched statistical copolymer. Bulk composition data show St enrichment compared to the feed ratio in all samples (see Table 4), while the observation of a narrow glass transition intermediate between PS and PBN2VN is consistent with a statistical sequence distribution.

# CONCLUSIONS

The data presented in this paper show that aromaticity results in well-matched reactivity ratios between styrene and a vinyl alcohol precursor. We report computational characterization of BN2VN aromaticity, including both structural parameters and NICS values. The BN naphthalene side chain influences radical stabilities in a manner similar to the phenyl side chain in styrene. The reactivity ratios  $r_1(\mathrm{BN2VN})$  and  $r_2(\mathrm{St})$  were determined by traditional linearization and modern NLLS statistical methods using two independent analytical techniques, elemental analysis, and UV—vis spectroscopy. Compared to other comonomer pairs (e.g., St—VAc or St—VSi), St and

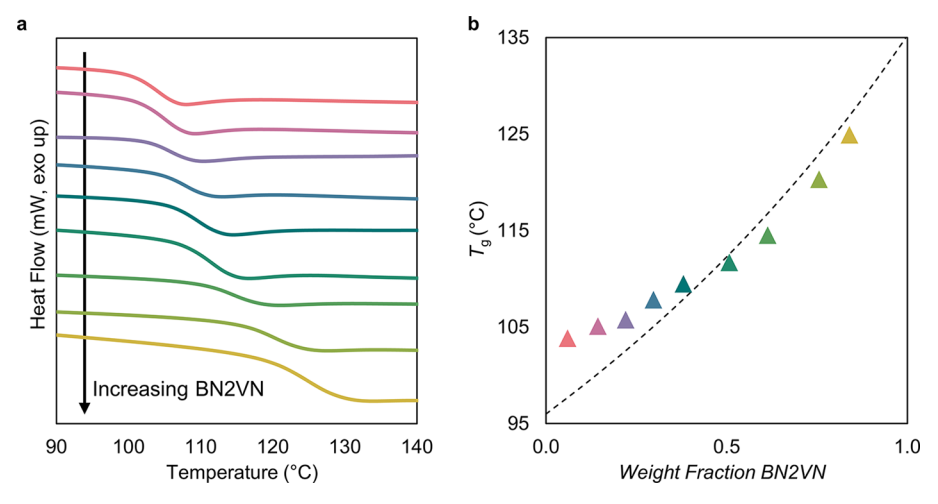


Figure 5. (a) Differential scanning calorimetry (DSC) thermograms of  $P(BN2VN_{4}\text{-}co\text{-}S_{103})$ ,  $P(BN2VN_{10}\text{-}co\text{-}S_{86})$ ,  $P(BN2VN_{15}\text{-}co\text{-}S_{81})$ ,  $P(BN2VN_{20}\text{-}co\text{-}S_{70})$ ,  $P(BN2VN_{25}\text{-}co\text{-}S_{61})$ ,  $P(BN2VN_{32}\text{-}co\text{-}S_{46})$ ,  $P(BN2VN_{38}\text{-}co\text{-}S_{35})$ ,  $P(BN2VN_{41}\text{-}co\text{-}S_{20})$ , and  $P(BN2VN_{39}\text{-}co\text{-}S_{11})$ . (b) Dependence of glass transition temperature ( $T_g$  point of inflection) on the weight fraction BN2VN in the copolymers. Predicted  $T_g$  (dashed line) calculated using the Fox equation.

Table 7. Comparison of Experimental and Predicted  $T_g$ 's

				-
entry	polymer	BN2VN <sup>a</sup> (wt %)	experimental $T_g^b$ (°C)	$ \begin{array}{c} \text{predicted} \\ T_{\text{g}}^{\ c} \ (^{\circ}\text{C}) \end{array} $
1	$P(BN2VN_4\text{-}co\text{-}S_{103})$	6.0	104	97
2	$P(BN2VN_{10}\text{-}co\text{-}S_{86})$	14	105	100
3	$P(BN2VN_{15}\text{-}co\text{-}S_{81})$	22	106	102
4	$P(BN2VN_{20}\text{-}co\text{-}S_{70})$	30	108	104
5	$P(BN2VN_{25}\text{-}co\text{-}S_{61})$	38	109	106
6	$P(BN2VN_{32}\text{-}co\text{-}S_{46})$	51	112	110
7	$P(BN2VN_{38}\text{-}co\text{-}S_{35})$	61	115	114
8	$P(BN2VN_{41}\text{-}co\text{-}S_{20})$	76	120	119
9	$P(BN2VN_{39}\text{-}co\text{-}S_{11})$	84	125	122

"Determined by UV—vis from  $\epsilon_{320}$  according to eq 4. "Point of inflection of the glass transition." Predicted  $T_{\rm g}$  calculated using the Fox equation."

BN2VN have the reactivity ratios closest to a random copolymerization.

Our results support the development of tailored styrenevinyl alcohol copolymer architectures, while minimizing the use of excess monomer. The relationship between organoborane structure and reactivity suggests design principles for well-matched reactivity between hybrid and organic vinyl monomers.

#### ASSOCIATED CONTENT

# **S** Supporting Information

The Supporting Information is available free of charge on the ACS Publications website at DOI: 10.1021/acs.macromol.8b01368.

Supplemental figures and tables, gel permeation chromatograms, copies of spectra (<sup>1</sup>H NMR, UV-vis, IR), details of computational procedures (PDF) Atomic coordinates of compounds studied by DFT (XYZ)

# AUTHOR INFORMATION

# **Corresponding Author**

\*E-mail klausen@jhu.edu (R.S.K.).

#### ORCID ®

Heidi L. van de Wouw: 0000-0002-2115-6325 Rebekka S. Klausen: 0000-0003-4724-4195

# **Notes**

The authors declare the following competing financial interest(s): A provisional patent based on this work has been filed (U.S. no. 62/573,065).

# ACKNOWLEDGMENTS

This material is based upon work supported by the National Science Foundation under Grant CHE-1752791. DFT calculations were conducted using scientific computing services at the Maryland Advanced Research Computing Center (MARCC). R.S.K. thanks the Alfred P. Sloan Foundation for a Sloan Research Fellowship, the American Academy of Arts and Sciences for the Mason Award for Women in the Chemical Sciences, and Johns Hopkins University for the Catalyst Award. We thank Prof. Howard E. Katz for DSC access and Dr. Maxime A. Siegler for X-ray crystallography. We thank Prof. David Haddleton (University of Warwick) for sharing the Contour program and Prof. Frank A. Leibfarth (University of North Carolina) for helpful discussions. A provisional patent based on this work has been filed (U.S. no 62/573,065).

## REFERENCES

- (1) Hallensleben, M. L.; Fuss, R.; Mummy, F. Polyvinyl Compounds, Others. In *Ullmann's Encyclopedia of Industrial Chemistry*; Wiley-VCH Verlag GmbH & Co. KGaA: Weinheim, Germany, 2015; pp 1–23.
- (2) Mayo, F. R.; Walling, C.; Lewis, F. M.; Hulse, W. F. Copolymerization. V. Some Copolymerizations of Vinyl Acetate. *J. Am. Chem. Soc.* **1948**, *70* (4), 1523–1525.
- (3) Mayo, F. R.; Lewis, F. M.; Walling, C. Copolymerization. VIII. The Relation Between Structure and Reactivity of Monomers in Copolymerization <sup>1</sup>. *J. Am. Chem. Soc.* **1948**, *70* (4), 1529–1533.
- (4) Franssen, N. M. G.; Reek, J. N. H.; de Bruin, B. Synthesis of Functional 'Polyolefins': State of the Art and Remaining Challenges. *Chem. Soc. Rev.* **2013**, *42* (13), 5809–5832.
- (5) Mayo, F. R.; Lewis, F. M. Copolymerization I. A Basis for Comparing the Behavior of Monomers in Copolymerization; the

Copolymerization of Styrene and Methyl Methacrylate. J. Am. Chem. Soc. 1944, 66 (1939), 1594–1601.

- (6) Odian, G. Principles of Polymerization, 4th ed.; WILEY-VCH Verlag: 2004.
- (7) van de Wouw, H. L.; Lee, J. Y.; Klausen, R. S. Gram-Scale Free Radical Polymerization of an Azaborine Vinyl Monomer. *Chem. Commun.* **2017**, *53*, 7262–7265.
- (8) van de Wouw, H. L.; Lee, J. Y.; Awuyah, E. C.; Klausen, R. S. A BN Aromatic Ring Strategy for Tunable Hydroxy Content in Polystyrene. *Angew. Chem., Int. Ed.* **2018**, *57* (6), 1673–1677.
- (9) Giustra, Z. X.; Liu, S.-Y. The State of the Art in Azaborine Chemistry: New Synthetic Methods and Applications. *J. Am. Chem. Soc.* **2018**, *140* (4), 1184–1194.
- (10) Campbell, P. G.; Marwitz, A. J. V.; Liu, S.-Y. Recent Advances in Azaborine Chemistry. *Angew. Chem., Int. Ed.* **2012**, *51* (25), 6074–6092.
- (11) Campbell, P. G.; Abbey, E. R.; Neiner, D.; Grant, D. J.; Dixon, D. A.; Liu, S.-Y. Resonance Stabilization Energy of 1,2-Azaborines: A Quantitative Experimental Study by Reaction Calorimetry. *J. Am. Chem. Soc.* **2010**, *132* (51), 18048–18050.
- (12) Ishibashi, J. S. A.; Marshall, J. L.; Mazière, A.; Lovinger, G. J.; Li, B.; Zakharov, L. N.; Dargelos, A.; Graciaa, A.; Chrostowska, A.; Liu, S.-Y. Two BN Isosteres of Anthracene: Synthesis and Characterization. J. Am. Chem. Soc. 2014, 136 (43), 15414–15421.
- (13) Davies, G. H. M.; Molander, G. A. Synthesis of Functionalized 1,3,2-Benzodiazaborole Cores Using Bench-Stable Components. *J. Org. Chem.* **2016**, *81* (9), 3771–3779.
- (14) Baranac-Stojanovic, M. Aromaticity and Stability of Azaborines. Chem. Eur. J. 2014, 20 (50), 16558–16565.
- (15) Gershoni-Poranne, R.; Stanger, A. Magnetic Criteria of Aromaticity. Chem. Soc. Rev. 2015, 44 (18), 6597–6615.
- (16) Su, K.; Remsen, E. E.; Thompson, H. M.; Sneddon, L. G. Syntheses and Properties of Poly(B-Vinylborazine) and Poly(Styrene-Co-B-Vinylborazine) Copolymers. *Macromolecules* **1991**, 24 (13), 3760–3766.
- (17) Llynch, A. T.; Sneddon, L. G. Transition-Metal-Promoted Reactions of Boron Hydrides. 12. Syntheses, Polymerizations, and Ceramic Conversion Reactions of B-Alkenylborazines. *J. Am. Chem. Soc.* 1989, 111 (16), 6201–6209.
- (18) Mirabelli, M. G. L.; Lynch, A. T.; Sneddon, L. G. Molecular and Polymeric Precursors to Boron-Based Ceramics. *Solid State Ionics* **1989**, 32–33, 655–660.
- (19) Staubitz, A.; Presa Soto, A.; Manners, I. Iridium-Catalyzed Dehydrocoupling of Primary Amine-Borane Adducts: A Route to High Molecular Weight Polyaminoboranes, Boron-Nitrogen Analogues of Polyolefins. *Angew. Chem., Int. Ed.* **2008**, 47 (33), 6212–6215
- (20) Ayhan, O.; Eckert, T.; Plamper, F. A.; Helten, H. Poly-(Iminoborane)s: An Elusive Class of Main-Group Polymers? *Angew. Chem., Int. Ed.* **2016**, 55 (42), 13321–13325.
- (21) Lorenz, T.; Lik, A.; Plamper, F. A.; Helten, H. Dehydrocoupling and Silazane Cleavage Routes to Organic-Inorganic Hybrid Polymers with NBN Units in the Main Chain. *Angew. Chem., Int. Ed.* **2016**, 55 (25), 7236–7241.
- (22) Lorenz, T.; Crumbach, M.; Eckert, T.; Lik, A.; Helten, H. Poly(p-Phenylene Iminoborane): A Boron–Nitrogen Analogue of Poly(p-Phenylene Vinylene). *Angew. Chem., Int. Ed.* **2017**, *56* (10), 2780–2784.
- (23) Staubitz, A. Generation of High-Molecular-Weight Polymers with Diverse Substituents: An Unusual Metal-Free Synthesis of Poly(Aminoborane)S. *Angew. Chem., Int. Ed.* **2018**, *57* (21), 5990–5992.
- (24) De Albuquerque Pinheiro, C. A.; Roiland, C.; Jehan, P.; Alcaraz, G. Solventless and Metal-Free Synthesis of High-Molecular-Mass Polyaminoboranes from Diisopropylaminoborane and Primary Amines. *Angew. Chem., Int. Ed.* **2018**, *57* (6), 1519–1522.
- (25) Helten, H. B=N Units as Part of Extended  $\pi$ -Conjugated Oligomers and Polymers. *Chem. Eur. J.* **2016**, 22 (37), 12972–12982.

(26) Baggett, A. W.; Guo, F.; Li, B.; Liu, S.-Y.; Jäkle, F. Regioregular Synthesis of Azaborine Oligomers and a Polymer with a Syn Conformation Stabilized by NH··· $\pi$  Interactions. *Angew. Chem., Int. Ed.* **2015**, *54* (38), 11191–11195.

- (27) Zhang, W.; Li, G.; Xu, L.; Zhuo, Y.; Wan, W.; Yan, N.; He, G. 9,10-Azaboraphenanthrene-Containing Small Molecules and Conjugated Polymers: Synthesis and Their Application in Chemodosimeters for the Ratiometric Detection of Fluoride Ions. *Chem. Sci.* 2018, 9 (19), 4444–4450.
- (28) Wan, W.-M.; Baggett, A. W.; Cheng, F.; Lin, H.; Liu, S.-Y.; Jäkle, F. Synthesis by Free Radical Polymerization and Properties of BN-Polystyrene and BN-Poly(Vinylbiphenyl). *Chem. Commun.* **2016**, 52, 13616–13619.
- (29) Thiedemann, B.; Gliese, P. J.; Hoffmann, J.; Lawrence, P. G.; Sönnichsen, F. D.; Staubitz, A. High Molecular Weight Poly(N-Methyl-B-Vinylazaborine) a Semi-Inorganic B—N Polystyrene Analogue. *Chem. Commun.* **2017**, *53*, 7258—7261.
- (30) Mulvaney, J. E.; Ottaviani, R. A.; Laverty, J. J. Preparation of Vinyl Boronate Copolymers and Reactions. *J. Polym. Sci., Polym. Chem. Ed.* **1982**, 20 (7), 1949–1952.
- (31) Woods, W. G.; Bengelsdorf, I. S.; Hunter, D. L. 2-Vinyl-4,4,6-Trimethyl-1,3,2-Dioxaborinane. I. Synthesis and Properties. *J. Org. Chem.* 1966, 31 (9), 2766–2768.
- (32) Chrostowska, A.; Xu, S.; Lamm, A. N.; Mazière, A.; Weber, C. D.; Dargelos, A.; Baylère, P.; Graciaa, A.; Liu, S.-Y. UV-Photoelectron Spectroscopy of 1,2- and 1,3-Azaborines: A Combined Experimental and Computational Electronic Structure Analysis. *J. Am. Chem. Soc.* **2012**, *134* (24), 10279–10285.
- (33) Abbey, E. R.; Lamm, A. N.; Baggett, A. W.; Zakharov, L. N.; Liu, S.-Y. Protecting Group-Free Synthesis of 1,2-Azaborines: A Simple Approach to the Construction of BN-Benzenoids. *J. Am. Chem. Soc.* **2013**, *135* (34), 12908–12913.
- (34) Marwitz, A. J. V.; Matus, M. H.; Zakharov, L. N.; Dixon, D. A.; Liu, S.-Y. A Hybrid Organic/Inorganic Benzene. *Angew. Chem., Int. Ed.* **2009**, 48 (5), 973–977.
- (35) Pan, J.; Kampf, J. W.; Ashe, A. J. The Ligand Properties of 2-Vinyl-1,2-Azaboratabenzene. *J. Organomet. Chem.* **2009**, 694 (7–8), 1036–1040.
- (36) Fazen, P. J.; Beck, J. S.; Lynch, A. T.; Remsen, E. E.; Sneddon, L. G. Thermally Induced Borazine Dehydropolymerization Reactions. Synthesis and Ceramic Conversion Reactions of a New High-Yield Polymeric Precursor to Boron Nitride. *Chem. Mater.* **1990**, 2 (2), 96–97.
- (37) Ihara, E.; Kurokawa, A.; Itoh, T.; Inoue, K. Homopolymerization and Copolymerization with Styrene of Various Alkoxyvinylsilanes and Oxidative Transformation of C-Si Bond in the Resulting Copolymers to Afford Poly[(Vinyl Alcohol)-Co-Styrene]S. *Polym. J.* **2008**, *40* (12), 1140–1148.
- (38) Ihara, E.; Kurokawa, A.; Itoh, T.; Inoue, K. A Novel Synthetic Strategy for Copolymers of Vinyl Alcohol: Radical Copolymerization of Alkoxyvinylsilanes with Styrene and Oxidative Transformation of C-Si(OR)2Me into C-OH in the Copolymers to Afford Poly(Vinyl Alcohol-Ran-Styrene)S. J. Polym. Sci., Part A: Polym. Chem. 2007, 45 (16), 3648–3658.
- (39) Yanai, T.; Tew, D. P.; Handy, N. C. A New Hybrid Exchange—Correlation Functional Using the Coulomb-Attenuating Method (CAM-B3LYP). *Chem. Phys. Lett.* **2004**, 393 (1–3), 51–57.
- (40) Latelli, N.; Ouddai, N.; Arotçaréna, M.; Chaumont, P.; Mignon, P.; Chermette, H. Mechanism of Addition-Fragmentation Reaction of Thiocarbonyls Compounds in Free Radical Polymerization. A DFT Study. *Comput. Theor. Chem.* **2014**, *1027*, 39–45.
- (41) Mazière, A.; Chrostowska, A.; Darrigan, C.; Dargelos, A.; Graciaa, A.; Chermette, H. Electronic Structure of BN-Aromatics: Choice of Reliable Computational Tools. *J. Chem. Phys.* **2017**, *147* (16), 164306.
- (42) Liu, Z.; Ishibashi, J. S. A.; Darrigan, C.; Dargelos, A.; Chrostowska, A.; Li, B.; Vasiliu, M.; Dixon, D. A.; Liu, S.-Y. The Least Stable Isomer of BN Naphthalene: Toward Predictive Trends

for the Optoelectronic Properties of BN Acenes. J. Am. Chem. Soc. 2017, 139 (17), 6082-6085.

- (43) Dewar, M. J. S.; Gleicher, G. J.; Robinson, B. P. Synthesis and Nuclear Magnetic Resonance Spectrum of 10,9-Borazaronaphthalene. *J. Am. Chem. Soc.* **1964**, *86* (24), 5698–5699.
- (44) Kranz, M.; Clark, T. Azaborines: An Ab Initio Study. J. Org. Chem. 1992, 57 (20), 5492–5500.
- (45) Ghosh, D.; Periyasamy, G.; Pati, S. K. Density Functional Theoretical Investigation of the Aromatic Nature of BN Substituted Benzene and Four Ring Polyaromatic Hydrocarbons. *Phys. Chem. Chem. Phys.* **2011**, *13* (46), 20627.
- (46) Klooster, W. T.; Koetzle, T. F.; Siegbahn, P. E. M.; Richardson, T. B.; Crabtree, R. H. Study of the N-H···H-B Dihydrogen Bond Including the Crystal Structure of BH3NH3 by Neutron Diffraction. *J. Am. Chem. Soc.* **1999**, *121* (27), 6337–6343.
- (47) Alcaraz, G.; Vendier, L.; Clot, E.; Sabo-Etienne, S. Ruthenium  $Bis(\sigma$ -B-H) Aminoborane Complexes from Dehydrogenation of Amine-Boranes: Trapping of H2B-NH2. *Angew. Chem., Int. Ed.* **2010**, 49 (5), 918–920.
- (48) Bosdet, M. J. D.; Piers, W. E. B-N as a C-C Substitute in Aromatic Systems. Can. J. Chem. 2009, 87 (1), 8-29.
- (49) Paetzold, P. New Perspectives in Boron-Nitrogen Chemistry I. *Pure Appl. Chem.* **1991**, *63* (3), 345–350.
- (50) McKinley, N. F.; O'Shea, D. F. Efficient Synthesis of Aryl Vinyl Ethers Exploiting 2,4,6-Trivinylcyclotriboroxane as a Vinylboronic Acid Equivalent. J. Org. Chem. 2004, 69 (15), 5087–5092.
- (51) Adler Yañez, R. A.; Kehr, G.; Daniliuc, C. G.; Schirmer, B.; Erker, G. Formation of a Dihydroborole by Catalytic Isomerization of a Divinylborane. *Dalt. Trans.* **2014**, *43* (28), 10794.
- (52) von Ragué Schleyer, P.; Maerker, C.; Dransfeld, A.; Jiao, H.; van Eikema Hommes, N. J. R. Nucleus-Independent Chemical Shifts: A Simple and Efficient Aromaticity Probe. *J. Am. Chem. Soc.* **1996**, *118* (26), 6317–6318.
- (53) Chen, Z.; Wannere, C. S.; Corminboeuf, C.; Puchta, R.; von Ragué Schleyer, P. Nucleus-Independent Chemical Shifts (NICS) as an Aromaticity Criterion. *Chemical Reviews*; American Chemical Society: 2005; pp 3842–3888.
- (54) London, F. Théorie Quantique Des Courants Interatomiques Dans Les Combinaisons Aromatiques. *J. Phys. Radium* **1937**, 8 (10), 397–409.
- (55) McWeeny, R. Perturbation Theory for the Fock-Dirac Density Matrix. *Phys. Rev.* **1962**, *126* (3), 1028–1034.
- (56) Ditchfield, R. Self-Consistent Perturbation Theory of Diamagnetism. Mol. Phys. 1974, 27 (4), 789-807.
- (57) Wolinski, K.; Hinton, J. F.; Pulay, P. Efficient Implementation of the Gauge-Independent Atomic Orbital Method for NMR Chemical Shift Calculations. *J. Am. Chem. Soc.* **1990**, *112* (23), 8251–8260.
- (58) Cheeseman, J. R.; Trucks, G. W.; Keith, T. A.; Frisch, M. J. A Comparison of Models for Calculating Nuclear Magnetic Resonance Shielding Tensors. *J. Chem. Phys.* **1996**, *104* (14), 5497.
- (59) Chrostowska, A.; Xu, S.; Mazière, A.; Boknevitz, K.; Li, B.; Abbey, E. R.; Dargelos, A.; Graciaa, A.; Liu, S.-Y. UV-Photoelectron Spectroscopy of BN Indoles: Experimental and Computational Electronic Structure Analysis. *J. Am. Chem. Soc.* **2014**, *136* (33), 11813–11820.
- (60) Del Bene, J. E.; Yáñez, M.; Alkorta, I.; Elguero, J. An Ab Initio Study of the Structures and Selected Properties of 1,2-Dihydro-1,2-Azaborine and Related Molecules. *J. Chem. Theory Comput.* **2009**, 5 (9), 2239–2247.
- (61) Catão, A. J. L.; López-Castillo, A. Stability and Molecular Properties of the Boron-Nitrogen Alternating Analogs of Azulene and Naphthalene: A Computational Study. *J. Mol. Model.* **2017**, 23 (4), 119
- (62) von Ragué Schleyer, P.; Jiao, H.; van Eikema Hommes, N. J. R.; Malkin, V. G.; Malkina, O. L. An Evaluation of the Aromaticity of Inorganic Rings: Refined Evidence from Magnetic Properties. *J. Am. Chem. Soc.* **1997**, *119* (51), 12669–12670.

(63) Islas, R.; Chamorro, E.; Robles, J.; Heine, T.; Santos, J. C.; Merino, G. Borazine: To Be or Not to Be Aromatic. *Struct. Chem.* **2007**, *18* (6), 833–839.

- (64) Wu, Y.-D.; Wong, C.-L.; Chan, K. W. K.; Ji, G.-Z.; Jiang, X.-K. Substituent Effects on the C-H Bond Dissociation Energy of Toluene. A Density Functional Study. *J. Org. Chem.* **1996**, *61* (2), 746–750.
- (65) Szwarc, M. The C-H Bond Energy in Toluene and Xylenes. *J. Chem. Phys.* **1948**, *16* (2), 128–136.
- (66) Blanksby, S. J.; Ellison, G. B. Bond Dissociation Energies of Organic Molecules. *Acc. Chem. Res.* **2003**, 36 (4), 255–263.
- (67) Ochterski, J. W. Thermochemistry in GaussianlGaussian.com.
- (68) Moad, G.; Solomon, D. H.; Johns, S. R.; Willing, R. I. Fate of the Initiator in the Azobis(Isobutyonitrile)-Initiated Polymerization of Styrene. *Macromolecules* **1984**, *17* (5), 1094–1099.
- (69) Joshi, R. M. A Brief Survey of Methods of Calculating Monomer Reactivity Ratios. J. Macromol. Sci., Chem. 1973, 7 (6), 1231–1245.
- (70) Scott, A.; Penlidis, A. Computational Package for Copolymerization Reactivity Ratio Estimation: Improved Access to the Errorin-Variables-Model. *Processes* **2018**, *6* (1), 8.
- (71) Van Herk, A. M.; Dröge, T. Nonlinear Least Squares Fitting Applied to Copolymerization Modeling. *Macromol. Theory Simul.* 1997, 6 (6), 1263–1276.
- (72) Fineman, M.; Ross, S. D. Linear Method for Determining Monomer Reactivity Ratios in Copolymerization. *J. Polym. Sci.* **1950**, 5 (2), 259–262.
- (73) Kelen, T.; Tüdös, F. Analysis of the Linear Methods for Determining Copolymerization Reactivity Ratios. I. A New Improved Linear Graphic Method. J. Macromol. Sci., Chem. 1975, 9 (1), 1–27.
- (74) Wrackmeyer, B. Carbon-13 NMR Spectroscopy of Boron Compounds. *Prog. Nucl. Magn. Reson. Spectrosc.* **1979**, 12 (4), 227–259.
- (75) Claudy, P.; Létoffé, J. M.; Camberlain, Y.; Pascault, J. P. Glass Transition of Polystyrene versus Molecular Weight. *Polym. Bull.* **1983**, 9–9 (4–5), 208–215.
- (76) Fox, T. G.; Flory, P. J. Second-Order Transition Temperatures and Related Properties of Polystyrene. I. Influence of Molecular Weight. *J. Appl. Phys.* **1950**, *21* (6), 581–591.
- (77) Höhne, G. W. H.; Hemminger, W. F.; Flammersheim, H.-J. Applications of Differential Scanning Calorimetry. In *Differential Scanning Calorimetry*; Springer: Berlin, 2003; pp 147–244.